Thermochimica Acta 475 (2008) 59–64

Contents lists available at ScienceDirect

Thermochimica Acta

journal homepage: www.elsevier.com/locate/tca

TGA–FTIR study of a lead zirconate titanate gel made from a triol-based sol–gel system

Anirban Chowdhury[a], Peter R. Thompson[b], Steven J. Milne[a,*]

[a] Institute for Materials Research, Houldsworth Building, University of Leeds, Leeds, LS2 9JT, UK
[b] Energy & Resources Research Institute, Houldsworth Building, University of Leeds, Leeds, LS2 9JT, UK

ARTICLE INFO

Article history:
Received 15 February 2008
Received in revised form 25 June 2008
Accepted 26 June 2008
Available online 5 July 2008

Keywords:
Sol–gel processes
Thermal decomposition
TGA–FTIR
Ferroelectric

ABSTRACT

A $Pb(Zr,Ti)O_3$ precursor gel made from a sol prepared using 1,1,1,-tris(hydroxymethyl)ethane, lead acetate and zirconium and titanium propoxides, stabilised with acetylacetone, was analysed using TGA–FTIR analysis. Decomposition under nitrogen (N_2) gave rise to evolved gas absorbance peaks at 215 °C, 279 °C, 300 °C and 386 °C, but organic vapours continued to be evolved, along with CO_2 and CO until ~950 °C. The final TGA step in N_2 is thought to relate to decomposition of an intermediate carbonate phase and the final elimination of residues of triol or acetylacetonate species which form part of the polymeric gel structure. By contrast, heating in air promoted oxidative pyrolysis of the final organic groups at ≤450 °C. In air, an intermediate carbonate phase was decomposed by heating at ~550 °C, allowing $Pb(Zr,Ti)O_3$ to be produced some 400 °C below the equivalent N_2 decomposition temperature.

1. Introduction

Lead zirconate titanate, $PbZr_xTi_{1-x}O_3$ (PZT), ceramics are of fundamental and practical interest because of their favourable dielectric, piezoelectric and ferroelectric properties. Thin film forms find potential applications in ferroelectric memories, bulk acoustic wave resonators and sensors [1]. A wide variety of preparation techniques have been employed to produce PZT thin films, such as sputtering, laser ablation, MOCVD (metalorganic chemical vapour deposition) and sol–gel [2–7].

In most sol–gel process for PZT, metal alkoxides and/or other metal-organic precursors are mixed in alcohol to form a stable sol, which on further reaction produces a polymeric gel network. For thin-film fabrication, the precursor sol is deposited onto a substrate by spin coating; subsequent heat-treatments to decompose the organic components of the metal-alkoxy gel are normally carried out on a hot-plate over the temperature range 200–400 °C. A final heat-treatment at 550–700 °C produces a crystalline, ferroelectric PZT film. The thickness of single-layer films produced by the early sol–gel routes was restricted to ~0.1 μm due to process-induced cracking. Several sol–gel routes have been reported subsequently, including two developed in this laboratory, which attain single-layer thickness values of ~0.4 or ~1 μm, making them potentially attractive for manufacturing films in the micron range, as fewer deposition-heating cycles are needed compared to earlier sol–gel systems [6–9]. One of the routes for thicker films involves forming a gel-precursor solution using a triol reagent [1,1,1-tris(hydroxymethyl)ethane, $CH_3C(CH_2OH)_3$] [6,7]. Information on the molecular structure of the starting sol has in the past been obtained using solution ^{13}C NMR spectroscopy which showed that oligomeric species were formed by molecular bridging of metal centers through the triol molecule. The triol exchanges initially for $-OC_3H_7$ ligands of the Ti and Zr pentanedionate modified starting propoxide reagents [6]. No detailed information is available on the thermochemistry of the gel to ceramic conversion. Here the results of TGA–FTIR experiments are reported. The approach has provided useful information on other sol–gel systems for producing ferroelectrics, for example $PbTiO_3$, $BaTiO_3$, $(Bi,La)_4Ti_3O_{12}$, $SrBi_2Nb_2O_9$ [10–12].

2. Experimental

Precursors from Sigma–Aldrich of zirconium *n*-propoxide, 70 wt% in *n*-propanol [$Zr(OC_3H_7)_4$]; titanium diisopropoxide bis(2,4-pentanedionate), [$Ti(OC_3H_7)_2(CH_3COCHCOCH_3)_2$] abbreviated TIAA (75 wt% solution in 2-propanol); lead (II) acetate trihydrate; and the triol gel-forming reagent 1,1,1,-tris(hydroxymethyl)ethane [$CH_3C(CH_2OH)_3$] abbreviated to 'THOME', were used to produce a $PbZr_{0.3}Ti_{0.7}O_3$ sol [6,7]. Firstly, $Zr(OC_3H_7)_4$ was added to 2,4-pentanedione (acetylacetone) under a N_2 atmosphere, the mixture was heated at 90 °C for 2 h, resulting in a golden solution. The TIAA,

* Corresponding author. Tel.: +44 113 343 2539; fax: +44 113 343 2384.
E-mail addresses: preac@leeds.ac.uk (A. Chowdhury), S.J.Milne@leeds.ac.uk (S.J. Milne).

0040-6031/$ – see front matter © 2008 Published by Elsevier B.V.
doi:10.1016/j.tca.2008.06.009

lead acetate trihydrate and THOME were added to the solution. The mixture was stirred at 70 °C for 4 h to obtain a stock solution and diluted thereafter with 2-methoxyethanol to a concentration 0.75 M. The sol was made with 10% molar excess of lead acetate, as this is a usual means of compensating for PbO loss by evaporation during thin-film heat-treatments. Thermogravimetric analysis (TGA) was conducted in flowing nitrogen and in air (Stanton & Redcroft TGA 1000, London, England). The gels for this purpose were obtained by drying the sol at 60 °C for 4 h on a hotplate stirrer. The TGA furnace was run at 20 °C min^{-1} until 950 °C. This was the maximum practicable working temperature of the apparatus; the sample was held at 950 °C for 20 min. The evolved gasses from the sample at different time/temperature combinations were analysed by Fourier transform infrared (FTIR) spectroscopy (NICOLET FTIR 560 spectrometer, Madison, WI) in the wavenumber range, 4000–400 cm^{-1}. Precision in measuring wavenumbers is estimated at ±10 cm^{-1}.

3. Results

3.1. Decomposition in nitrogen

A standard TGA plot of the PZT precursor gels heated in N_2, Fig. 1a, shows the main mass loss to occur below 500 °C, equating to 48 mass% of the original dried gel sample. The four main mass loss stages, following the 60 °C pre-treatment, occurred over the approximate temperature ranges: 130–250 °C, 250–300 °C, 300–350 °C and 350–450 °C. A small, gradual loss of around a further 2 mass% occurred from ~750 °C to the maximum temperature studied, 950 °C. The corresponding Gram–Schmidt plot, showing the variation in the total absorbance of evolved gasses as a function of time/temperature, Fig. 2a, indicated peaks at 107 °C (very faint), 215 °C, 279 °C (with a shoulder at 300 °C), 386 °C and a broad, low intensity absorbance over the temperature range 750–950 °C, which extended into the hold period at 950 °C.

The FTIR spectra of the vapours evolved at temperatures corresponding to the peaks on the Gram–Schmidt plot are presented in Fig. 3, and the principal features are described below. Peak assignments were carried out with reference to standard texts [13–15] and instrument software (Nicolet Vapor Phase Library, Madison, WI).

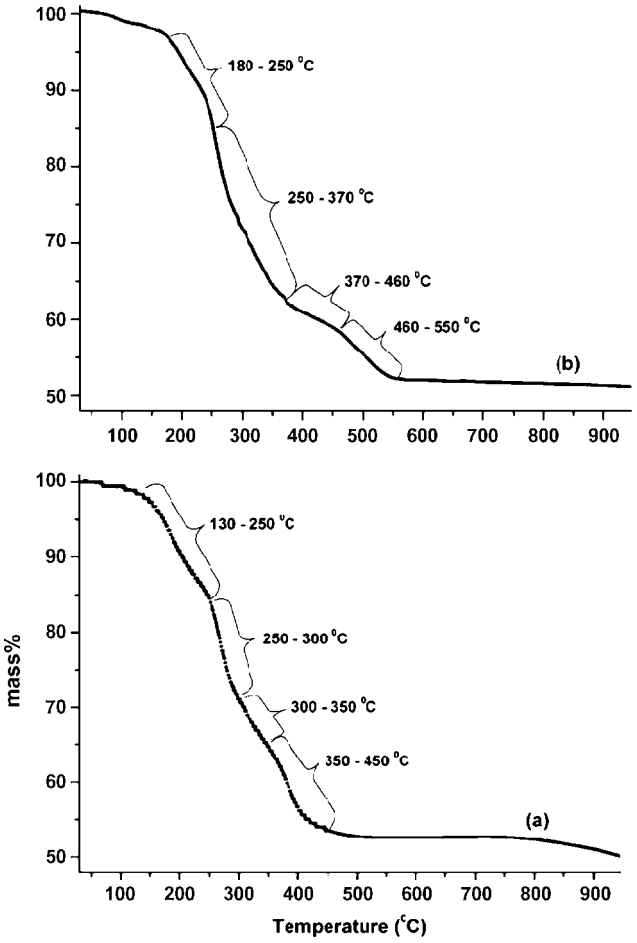

Fig. 1. TGA pattern of the dried triol-based $Pb(Zr_{0.3}Ti_{0.7})O_3$ sol carried out (a) in N_2 and (b) in air.

107 °C (Fig. 3a): Only very faint peaks (absorbance < 0.005) appeared in the FTIR spectrum at this temperature, implying that only a small volume of vapour was released, in agreement with the very low intensity of the Gram–Schmidt peak (Fig. 2a). Broad

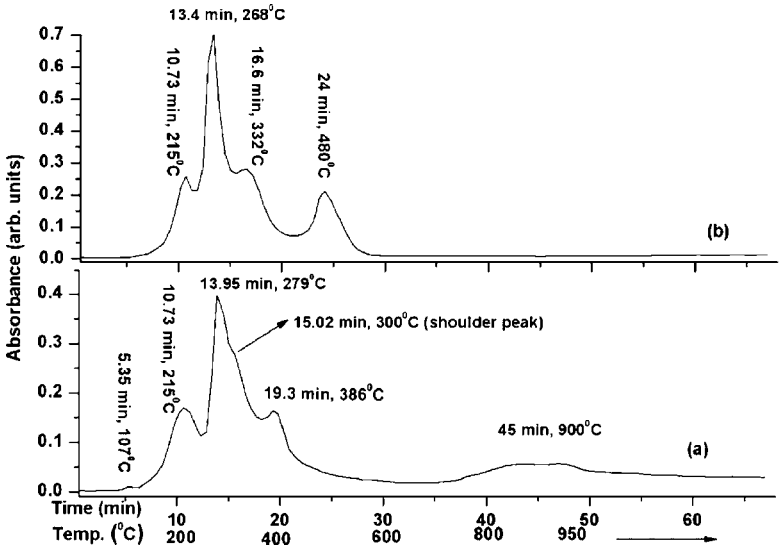

Fig. 2. FTIR Gram–Schmidt plot of the dried sol for (a) N_2 and (b) air.

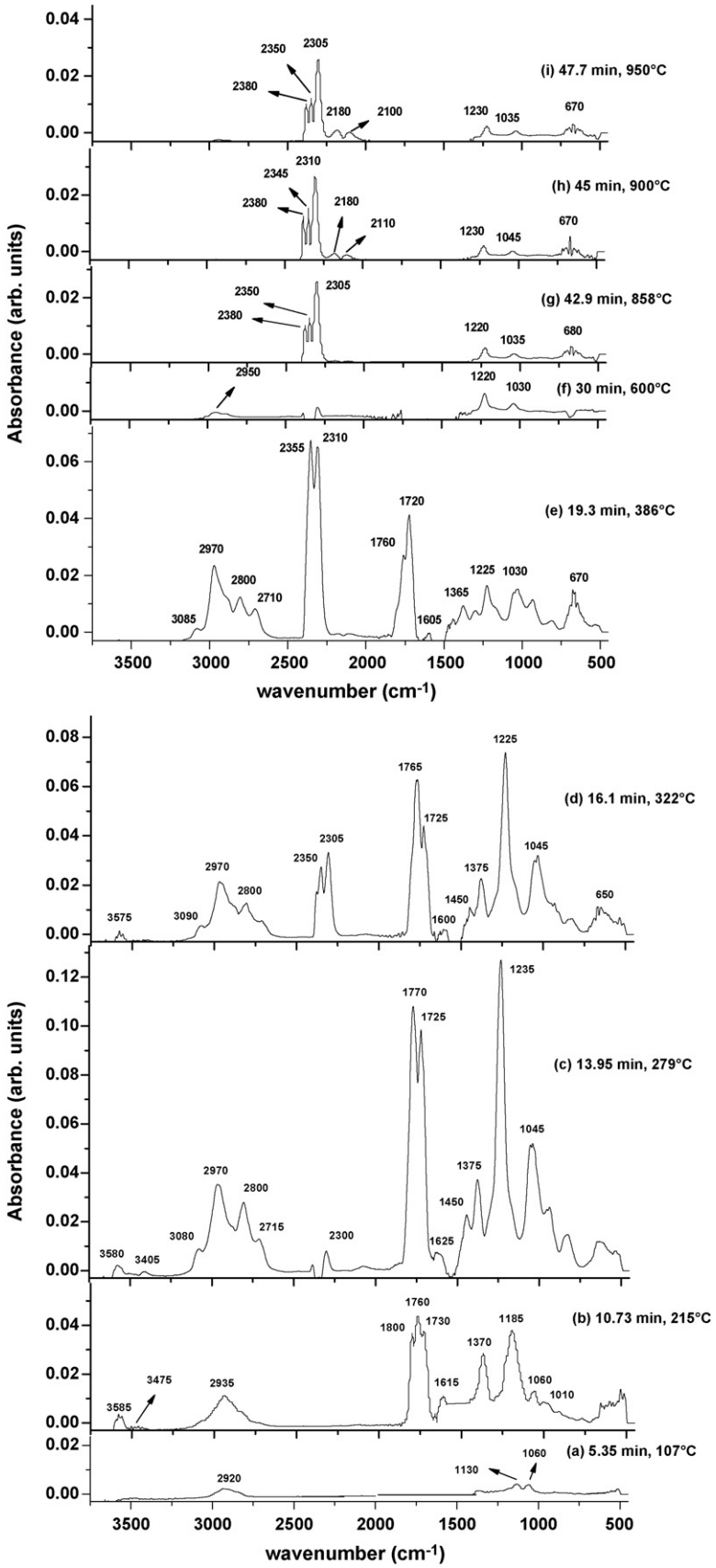

Fig. 3. FTIR spectra of the evolved gases from the dried $Pb(Zr_{0.3}Ti_{0.7})O_3$ sol during the TGA experiment at different time/temperatures in nitrogen: (a) 107 °C, (b) 215 °C, (c) 279 °C, (d) 322 °C, (e) 386 °C, (f) 600 °C, (g) 858 °C, (h) 900 °C and (i) 950 °C.

absorbance around 2900 cm^{-1}, due to aliphatic C–H stretches, and peaks around 1130 cm^{-1} and 1060 cm^{-1} due to C–O stretching vibration are typical of alcohols. Very faint absorbance due to O–H stretch was present around 3500 cm^{-1}. The weak Gram–Schmidt peak is therefore probably due to small amounts of alcohol solvent which were not eliminated fully during the prolonged preliminary heat-treatment at 60 °C.

215 °C (Fig. 3b): Absorbances centered at 3585 cm^{-1} and 3475 cm^{-1} signify O–H stretching. Three strong carbonyl stretches (C=O) exist at 1800 cm^{-1}, 1760 cm^{-1} and 1730 cm^{-1}. The former two peaks could be due to acetic acid, or other similar carboxylic acid. Acetic acid could arise as a by-product of ligand exchange reactions involving the acetate groups originating from the lead acetate starting component, and the triol reagent [6]. The lower wavenumber carbonyl peak(s) could signify other carboxylic acid or/and ester groups. However, ketone/aldehyde groups or acid anhydrides cannot be excluded on the basis of IR data. The peak at 1370 cm^{-1} (medium) is assigned to $-CH_3$ bending and/or O–H deformation of RCOOH. The 1185 cm^{-1} (strong) absorbance is associated with the corresponding C–O stretch of carboxylic acid. The peaks at 1060 cm^{-1} and 1010^{-1} cm are attributed to C–O vibrations.

279 °C (Fig. 3c): The ~1800 cm^{-1} absorbance is no longer present. An ester is inferred by carbonyl bands at 1770 cm^{-1} and 1725 cm^{-1}, together with a very strong peak at 1235 cm^{-1} typical of the stretching vibration of the C–O–C group within an ester. An equivalent stretch in the 215 °C pattern could have been masked by overlap by the neighbouring strong 1185 cm^{-1} peak. The fact that the 1235 cm^{-1} peak is the strongest in the pattern, and there is a 1045 cm^{-1} peak of medium intensity could indicate an ether or vinyl ether ($R_2C{=}CH{-}O{-}CR_3$) to coexist with an ester. The ether group would give rise to the asymmetrical C–O–C stretching between 1275 and 1200 cm^{-1} and symmetric stretching at 1075–1020 cm^{-1}. Overlap of peaks from ether and ester could account for the very high intensity of the 1235 cm^{-1} peak. For a vinyl ether, an accompanying C=C stretch at ~1660–1610 cm^{-1} is expected; a peak at ~1625 cm^{-1} appears in Fig. 3c. A weak peak at 2300 cm^{-1} is inconclusive – it could indicate the onset of CO_2 formation at this temperature, and the commencement of pyrolytic decomposition, involving cleavage of covalent bonds. Alternatively it could be due to drift in the background correction. Multiple peaks around 3000 cm^{-1} arise from various C–H and C–C stretches; OH groups are also indicated at higher wavenumbers.

322 °C (Fig. 3d): This temperature is included as it lies just beyond the shoulder to the previous peak in the Gram–Schmidt plot (Fig. 2a). There is a much higher CO_2 absorbance than at 279 °C, with peaks at 2350 cm^{-1} and 2305 cm^{-1} visible. This suggests the shoulder to the main Gram–Schmidt peak is due to an increased rate of CO_2 production, indicating a major pyrolytic decomposition step. The remaining peaks were similar to the 279 °C spectrum indicating no significant changes in the other decomposition products.

386 °C (Fig. 3e): The most intense peaks are the CO_2 stretches at 2355 cm^{-1} and 2310 cm^{-1}. There is no evidence of O–H stretch, but carbonyl peaks are still present at 1760 cm^{-1} and 1720 cm^{-1}. The diminution of the ~1225 cm^{-1} ester, or ether stretch, relative to the lower temperature spectra, points to ketone/aldehydes as the main contribution to the total carbonyl absorbance at this temperature. If esters are no longer present, ether would be the source of the 1225 cm^{-1} (and 1030 cm^{-1}) peak. The peaks around 670 cm^{-1} are due to bending modes of CO_2.

600 °C (Fig. 3f): This temperature lies in a region of apparently constant sample mass by TGA (Fig. 1a). However, vapours are detected by FTIR which suggest minor amounts of ether (1220 cm^{-1} and 1030 cm^{-1}). It is uncertain whether the small blip around the CO_2 stretch region is indicative of CO_2, or an anomaly related to drift in the background correction carried out at the start of the run.

858 °C, 900 °C, 950 °C (Fig. 3g–i): The main absorbances are from CO_2 at 2350 and 2305 cm^{-1} but very faint peaks at 2180 cm^{-1} and 2110 cm^{-1} signify some carbon monoxide production, which increases in amount with rising temperature. A peak at 2380 cm^{-1} (medium) is of uncertain origin; it may be due to a C≡N or C=N bond of a nitrile or isocyanate species indicating reaction between evolved organic species and the N_2 carrier gas. The enhanced intensity of the peak at 2305–2310 cm^{-1} relative to a standard CO_2 couplet suggests overlap of the peak with a second peak of similar wavenumber, which could be from an alkyl isocyanate R–N=C=O. No carbonyl species or OH containing species are detected. A pair of peaks at 1230 cm^{-1} and 1045 cm^{-1} with a characteristic intensity ratio of symmetric and asymmetric C–O–C stretches of ether is still present, confirming that the high temperature TGA mass loss at 750–950 °C was not due simply to inorganic carbonate decomposition.

3.2. Decomposition in air

The basic TGA plot, Fig. 1b, in air shows mass loss up to ~ 550 °C; above this temperature there was a slight deviation but the gradient remained the same at all temperatures, suggesting baseline drift. However, the possibility of some PbO volatilization in either sample cannot be excluded. The principal mass loss stages occurred at approximately 180–250 °C, 250–370 °C, 370–460 °C, 460–550 °C. The Gram–Schmidt plot, Fig. 2b, shows peaks at 215 °C, 268 °C, 332 °C and 480 °C, but no distinct peak in the temperature range 370–460 °C for which a small change in mass was recorded (Fig. 1b). The N_2 run showed a small peak at 107 °C due to alcohol evaporation; the absence of a corresponding peak in air is probably due to slight variability in gel drying conditions prior to the TGA runs.

215 °C (Fig. 4a): This first decomposition stage liberates CO_2 (peaks at 2355 cm^{-1} and 2305 cm^{-1}) indicating oxidative decomposition, causing the cleavage of organic bonds at much lower temperatures than for pyrolysis in N_2. The remaining peaks include weak OH stretch of H_2O, and a broad absorbance in the carbonyl region, indicative of overlapping peaks due to carboxylic acid/ester or ketone/aldehyde products. Associated very faint aliphatic C–H peaks are present.

268 °C (Fig. 4b): This pattern is also dominated by CO_2 absorbance. There is a narrowing of the wavelength range of the carbonyl stretches indicating a different combination of carbonyl products, relative to 215 °C. A 1240 cm^{-1} peak (medium) and a 1050 cm^{-1} peak (weak) are suggestive of ester or ether.

332 °C (Fig. 4c): The peaks due to organic vapours are much reduced compared to the previous temperature, with CO_2 very dominant. The intensity of OH stretch is similar to the two preceding spectra.

418 °C (Fig. 4d): TGA mass loss occurred between 370 and 460 °C without giving rise to a distinctive Gram–Schmidt peak, the FTIR pattern confirmed that only CO_2 was produced in this decomposition step.

480 °C (Fig. 4e): Again only CO_2 peaks are present. The absence of organic species in the 418 °C and 480 °C FTIR patterns indicate that the final TGA steps at 370–460 °C and 450–550 °C (Fig. 1b) most probably represent decomposition of metal (lead) carbonates which had formed due to reaction of the evolving metal oxides with the CO_2 evolved from gel oxidative pyrolysis (and with CO_2 present in the air carrier gas). An FTIR spectrum of a gel-sample heat-treated at 450 °C for 10 min is shown in Fig 5. The peaks at 1435 cm^{-1} and 1320 cm^{-1} are consistent with the presence of inorganic lead carbonate [16]. The existence of a peak at 3400 cm^{-1} suggests a hydrated carbonate phase may be formed. Fig. 5 also shows the FTIR pattern of a sample of gel heated at 450 °C in nitrogen, which is discussed below.

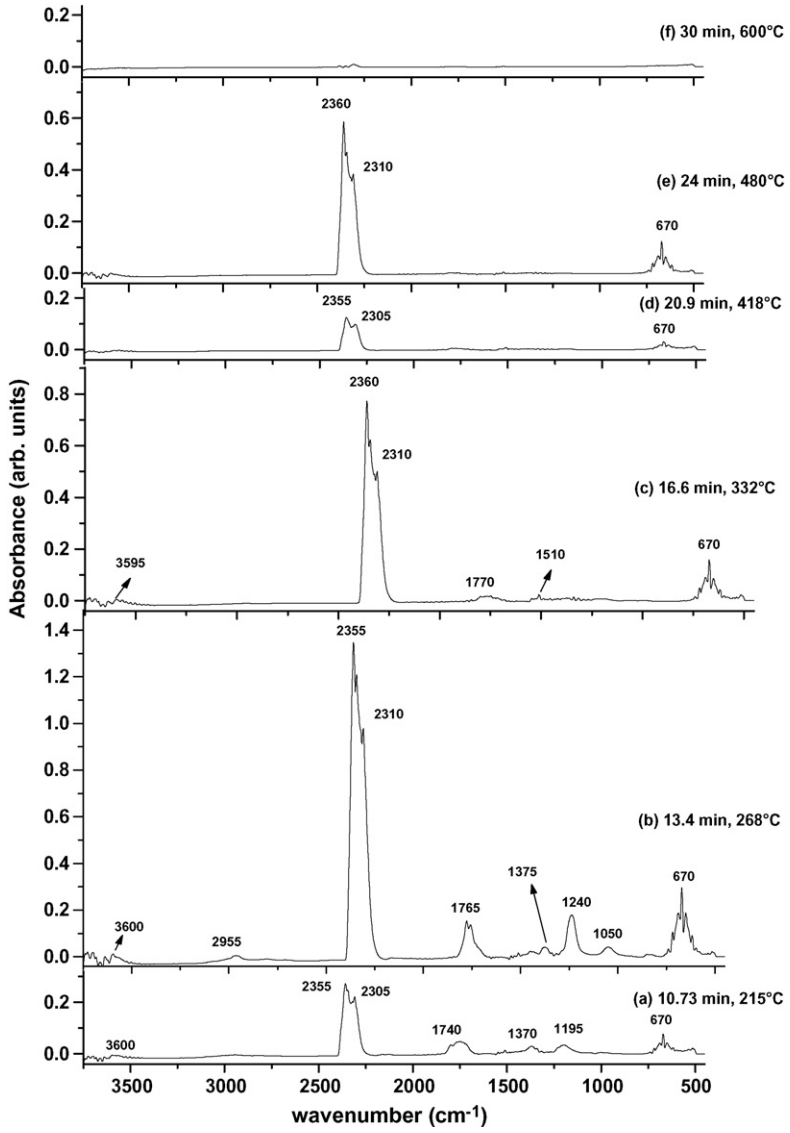

Fig. 4. FTIR spectra of the evolved gases from the dried $Pb(Zr_{0.3}Ti_{0.7})O_3$ sol during the TGA experiment at different time/temperatures in air: (a) 215 °C, (b) 268 °C, (c) 332 °C (d) 418 °C (e) 480 °C, (f) 600 °C (blip at ~2300 cm^{-1} in 600 °C pattern is linked to air compensation procedure).

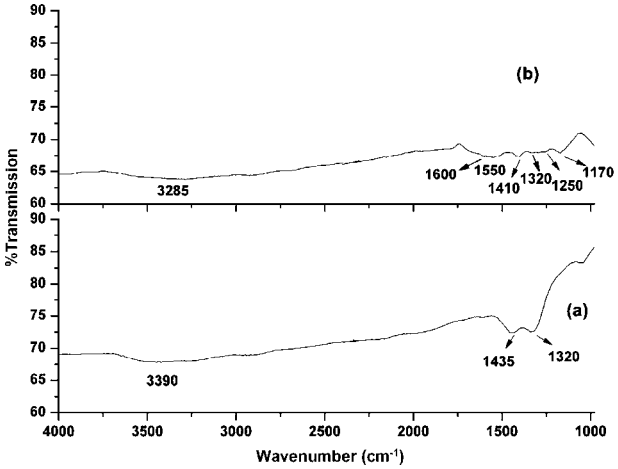

Fig. 5. FTIR spectra of the dried $Pb(Zr_{0.3}Ti_{0.7})O_3$ gel heat-treated at 450 °C for 10 min (a) in air and (b) in nitrogen.

600 °C (Fig. 4f): An FTIR pattern at 600 °C (Fig. 4f) confirmed there to be no further volatilization (the minute deviation in the CO_2 region is most probably due to baseline drift in the background correction.

4. Discussion

Background studies on the molecular structure of starting sols [6] indicated that propoxy ligands undergo ligand exchange more readily than the chelating acetylacetonate species on the Ti and Zr starting species The results indicated that the molecular structure of the starting gels is based on a framework of metal centers linked via THOME molecules, with acetylacetonate chelating groups chemically bound within the structure.

Comparing the two sets of thermal decomposition results, there is a marked difference in the decomposition of the triol PZT gels under nitrogen and air atmospheres. In nitrogen, the formation/evaporation of carboxylic acids, esters and/or ketone by-products of sol–gel synthesis, trapped in the gel structure, occur during the first TGA mass loss step commencing at around ~180 °C,

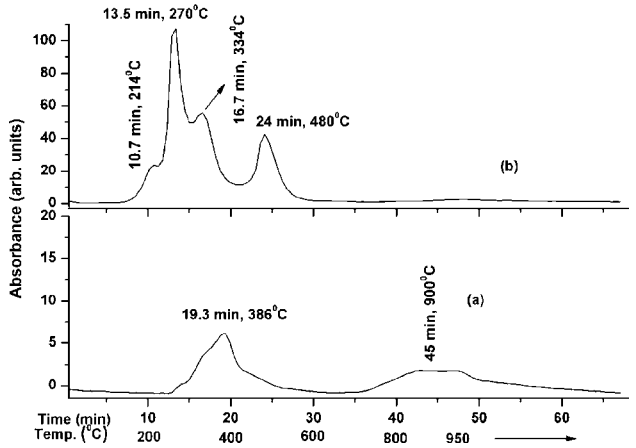

Fig. 6. CO_2 chemigram plot of the dried sol for (a) N_2 and (b) air. (*Note*: Different absorbance scales; a, b.)

but cleavage of organic covalent bonds (inferred from CO_2 formation) occurs mainly in the temperature range ~300–450 °C. Above 450 °C there appears from TGA to be no further decomposition until around 750 °C, however, FTIR at 600 °C shows that very small amounts of ether and possibly CO_2 are being produced in this region under nitrogen, but the levels are too low to record as a change in mass in TGA plots. At higher temperatures where a TGA mass loss is evident, namely ~750–950 °C (and probably slightly higher temperatures) CO_2 is clearly evident together with carbon monoxide and ether. The suspected appearance of nitrile or cyanate species in the highest temperature samples may be explained by reaction between the specific combination of organic vapours, CO_2 and the carrier N_2 gas. The role of Pb and other metal species in producing these species is uncertain.

In air, more inorganic carbonate (hydrated) phase forms at intermediate decomposition temperatures than in nitrogen, as indicated by comparison of the FTIR spectra of gel samples heated at 450 °C, Fig. 5. Not only are carbonate peaks of much lower intensity in the nitrogen sample, a number of organic functional groups are also indicated. Evidence of organic species includes a broad absorption from ~1750 cm^{-1} to ~1450 cm^{-1} with peaks at 1600 cm^{-1} and 1550 cm^{-1} in the region associated with metal carboxylate ions, C=C stretches and/or enol form of diketone (e.g. acetylacetonate). Peaks at 1250 cm^{-1} and 1170 cm^{-1} are consistent with C–O stretches. Presumably, the larger proportion of carbonate phase in gel residues after heating in air is a result of more CO_2 being produced during the preceding pyrolysis stages, as highlighted in the CO_2 chemigram of Fig. 6, as well as by reaction with CO_2 present in the carrier gas. The TGA plot (Fig. 1), in conjunction with FTIR data, infers the carbonate phase in the air sample to decompose in the temperature range 460–550 °C. Under nitrogen, a carbonate phase is also formed (in smaller quantity) but decomposes at much higher temperatures, up to ~950 °C. It is speculated, based on earlier studies of gel formation reactions [6] that the organic vapours formed at high temperatures under N_2 originate from the final decomposition of THOME molecules, which form part of the polymeric chain, and/or acetylacetonate residues within the gel. The vinyl ether which is tentatively identified here could be a reaction product of the thermolysis of these groups.

It is possible that similar ethers are produced at lower temperatures, for example the 279 °C spectrum also exhibits the characteristic intensity ratio and frequencies of the asymmetric and symmetric vinyl ether stretches at 1235 cm^{-1} and 1045 cm^{-1}. These may form from free (excess) THOME, not involved in the gel formation, or from less strongly bound acetylacetonate groups. In air the THOME and acetylacetonate groups are eliminated more easily, since these conditions promote oxidative decomposition. Hence there is no evidence of ether in the FTIR pattern at 332 °C (Fig. 5c).

In the past, PZT films produced by the triol (THOME) sol–gel route have normally been processed using only one hot-plate treatment at a temperature in the range 300–400 °C, or occasionally with a 200 °C pre-treatment. Although, the kinetics of gel and thin-film decomposition will differ, the present results suggest a decrease in process-induced stresses, and thus an increase in film crack-resistance may be possible by increasing the number of hot-plate heat-treatments such that they coincide with the main TGA mass loss steps. In future, four treatments involving temperatures close to those highlighted in Fig. 2b should be investigated for the purpose of minimising structural disruption associated with gas evolution.

5. Conclusions

TGA–FTIR of a PZT gel prepared from lead acetate, and acetylacetonate-stabilised titanium and zirconium propoxides using a triol [$CH_3C(CH_2OH)_3$] gel-forming agent was performed in nitrogen and air. Decomposition in air involved four steps, with the final one occurring at 450–550 °C and associated with inorganic carbonate decomposition. Gel powders heated under N_2 gave rise to a more complex decomposition sequence culminating at 750–950 °C in the decomposition of carbonate and probably residual triol or acetylacetonate residues. The reaction of these organic vapours in N_2, generated an additional product thought to be a nitrile and/or isocyanate species.

References

[1] G.H. Haertling, J. Am. Ceram. Soc. 82 (1999) 797–818.
[2] R. Takayama, Y. Tomita, J. Appl. Phys. 65 (1989) 1666–1670.
[3] O. Auciello, L. Mantese, J. Duarte, X. Chen, S.H. Rou, A.I. Kingon, A.F. Schreiner, A.R. Krauss, J. Appl. Phys. 73 (1993) 5197–5207.
[4] C.M. Foster, G.R. Bai, R. Csencsits, J. Vetrone, R. Jammy, L.A. Wills, E. Carr, J. Amano, J. Appl. Phys. 81 (1997) 2349–2357.
[5] K.D. Budd, S.K. Dey, D.A. Payne, Br. Ceram. Proc. 36 (1985) 107–121.
[6] N. Sriprang, D. Kaewchinda, J.D. Kennedy, S.J. Milne, J. Am. Ceram. Soc. 83 (2000) 1914–1920.
[7] M. Naksata, R. Brydson, S.J. Milne, J. Am. Ceram. Soc. 86 (2003) 1560–1566.
[8] Y.L. Tu, S.J. Milne, J. Mater. Res. 11 (1996) 2556–2564.
[9] Y.-L. Tu, M.L. Calzada, N.J. Phillips, S.J. Milne, J. Am. Ceram. Soc. 79 (1996) 441–448.
[10] A. Hardy, K. Van Werde, G. Vanhoyland, M.K. Van Bael, J. Mullens, L.C. Van Poucke, Thermochim. Acta 397 (2003) 143–153.
[11] J. Mullens, K. Van Werde, G. Vanhoyland, R. Nouwen, M.K. Van Bael, L.C. Van Poucke, Thermochim. Acta 392–393 (2002) 29–35.
[12] D. Nelis, D. Mondelaers, G. Vanhoyland, A. Hardy, K. Van Werde, H. Van den Rul, M.K. Van Bael, J. Mullens, L.C. Van Poucke, J. D'Haen, Thermochim. Acta 426 (2005) 39–48.
[13] R.M. Silverstein, F.X. Webster, Spectrometric Identification of Organic Compounds, 6th ed., New York, 1997.
[14] G. Socrates, Infrared and Raman Characteristic Group Frequencies: Tables and Charts, 3rd ed., Wiley, Chichester, 2001.
[15] D.H. Williams, I. Fleming, Spectroscopic Methods in Organic Chemistry, 4th ed., McGraw-Hill, London, 1990.
[16] J.M. Hunt, M.P. Wisherd, L.C. Bonham, Anal. Chem. 22 (1950) 1478–1497.